Research paper

Mild blast-related TBI in a mouse model alters amygdalar neurostructure and circuitry

Whitney A. Ratliff[a,b,*], Ronald F. Mervis[c,d], Bruce A. Citron[a,b,e,f], Brian Schwartz[g], Vardit Rubovitch[g], Shaul Schreiber[h,i,j], Chaim G. Pick[g,j,k]

[a] Bay Pines VA Healthcare System, Research and Development, 151, Bldg. 22 Rm. 123, 10000 Bay Pines Blvd, Bay Pines, FL 33744, USA
[b] Department of Molecular Medicine, USF College of Medicine, 12901 Bruce B. Downs Blvd, MDC 7, Tampa, FL 33612, USA
[c] NeuroStructural Analytics, Inc., Columbus, OH, USA
[d] Center for Aging and Brain Repair, Department of Neurosurgery and Brain Repair, University of South Florida Morsani College of Medicine, 2 Tampa General Circle, Tampa, FL 33606, USA
[e] VA New Jersey Health Care System, Research & Development, Mailstop 15, Bldg. 16, Rm. 16-176, 385 Tremont Ave, East Orange, NJ 07018, USA
[f] Department of Pharmacology, Physiology & Neuroscience, Rutgers- New Jersey Medical School, 185 South Orange Ave., Newark, NJ 07101, USA
[g] Department of Anatomy and Anthropology, Sackler School of Medicine, Tel Aviv University, Tel Aviv 69978, Israel
[h] Department of Psychiatry, Tel Aviv Sourasky Medical Center, Tel Aviv 64239, Israel
[i] Department of Psychiatry, Tel Aviv University Sackler Faculty of Medicine, Tel Aviv 64239, Israel
[j] Sagol School of Neuroscience, Tel Aviv University, Tel Aviv 69978, Israel
[k] Dr. Miriam and Sheldon G. Adelson Chair, Center for the Biology of Addictive Diseases, Tel Aviv University, Tel Aviv 69978, Israel

ARTICLE INFO

ABSTRACT

Traumatic brain injury (TBI) continues to be a signature injury of our modern conflicts. Due in part to increased use of improvised explosive devices (IEDs), we have seen blast trauma make up a significant portion of TBIs sustained by deployed troops and civilians. In addition to the physical injury, TBI is also a common comorbidity with post-traumatic stress disorder (PTSD). Previous research suggests that PTSD is often associated with increased signaling within the amygdala, leading to feelings of fear and hyperarousal. In our study, we utilized a mouse model of mild blast-related TBI (bTBI) to investigate how TBI induces changes within the amygdala, which may provide favorable conditions for the development of PTSD. To do this, we performed Golgi staining on the stellate neurons of the basolateral amygdala and quantified dendritic amount, distribution, and complexity. We found increases in dendritic branching and in the density of dendritic spines in injured mice. Increases in spine density appears to be primarily due to increases in memory associated mushroom type dendritic spines. These changes observed in our bTBI model that are consistent with chronic stress models, suggesting an important connection between the physical changes induced by TBI and the neurological symptoms of PTSD.

1. Introduction

Traumatic brain injury (TBI) is characterized by an acute brain injury which occurs as a result of external forces applied to the head. Some of the highest rates of incidence of TBI occur among military personnel and a significant proportion of these injuries result from being exposed to the shock wave associated with an explosive blast. The increased use of improvised explosive devices (IEDs) has led to blast TBI (bTBI) becoming a signature affliction of both combatants and civilians in recent conflicts. Importantly, TBI is also a major risk factor for the development of Post-Traumatic Stress Disorder (PTSD) (Tanev et al. 2014).

The essential feature of posttraumatic stress disorder is the development of characteristic symptoms following exposure to one or more traumatic events. Diagnostic criteria for PTSD include a history of exposure to a traumatic event that meets specific stipulations and symptoms from each of four symptom clusters: intrusion, avoidance, negative alterations in cognitions and mood, and alterations in arousal and reactivity (American Psychiatric Association 2013). PTSD has a long descriptive history, with an early definition closely linked to the experiences that soldiers suffered in combat. Before the PTSD diagnosis existed, many features of the syndrome following the terrible carnage of

trench warfare during World War I were recognized, and led to systematic descriptions of the syndrome under names such as "shell shock" or "combat fatigue" (Andreasen 2014) – mixing the effects of 'psychological trauma' (PTSD) with those induced by explosive blasts.

However, even though there still is some controversy regarding diagnostic criteria for minimal traumatic brain injury (mTBI) when blunt trauma to the head is involved (Jackson et al. 2016), much less is known regarding blast-induced mTBI. There is research in both humans and animals to suggest that blast-induced TBI can result in behavioral symptoms, such as anxiety, that are indicative of PTSD, in addition to neural injury (Bogdanova and Verfaellie, 2012; Kaplan et al. 2018; Rachmany et al. 2017; Rubovitch et al. 2011; Sajja et al. 2015). The relationship between mTBI and some manifestations of PTSD can end in the erroneous misidentification of mTBI and the diagnosis of PTSD in individuals that do not have it – a rather problematic condition that may hamper the administration of an efficacious treatment suitable for one condition but not for the other one.

A fairly substantial body of knowledge has been accumulated and published in the last decade and a half, detailing the effects of trauma exposure (either PTSD, or mTBI, or both) on brain morphology (mainly the impact on the hippocampus and to a lesser extent on the amygdala structure and function) (Admon et al. 2013; Ahmed-Leitao et al. 2016). The amygdala's involvement in PTSD derives from its major role in fear conditioning and fear extinction activities (VanElzakker et al. 2014). In patients with PTSD the amygdala is "burning" with hyperactivity in reaction to trauma-related cues (Shin and Liberzon 2010) and this "burning" pattern is characteristically demonstrated on functional imaging modalities (i.e. fMRI, PET, SPECT) (Pitman et al. 2001; Rauch et al. 2006; Sartory et al. 2013; Seedat et al. 2004). Changes in the volume of the amygdala may follow exposure to trauma, or precede it (then, predisposing for the development of PTSD) (Admon et al. 2009).

Given the important role of the amygdala in PTSD and its common comorbidity with TBI, it stands to reason that TBI may be influencing the amygdala in such a way that facilitates the development of PTSD. In fact, one recent study of a rat model of midline fluid percussion injury did note dendritic hypertrophy within the basolateral amygdala following injury (Hoffman et al. 2017). There remains, however, a dearth of information on how the amygdala is affected by injury, especially with respect to explosive blasts. One of the best ways to examine the effect of TBI on the amygdala is by utilizing Golgi staining. Golgi staining is a silver staining technique which has been used for over a century to allow whole individual neurons to be visualized. This powerful tool lends itself to numerous analysis techniques to examine the cellular effects of any number of conditions within the brain (Koyama et al. 2013). Importantly, Golgi staining allows for specific analysis of

the dendrites of individual neurons without interference of neighboring neurons. We are able to evaluate dendritic complexity, density, and branching, in addition to analyzing dendritic spines and spine subtypes. Several previous studies have shown how TBI significantly alters these dendritic measures in ways that would not be detected using other traditional analyses (Casella et al. 2014; Gao et al. 2011; Saykally et al. 2017; Winston et al. 2013).

In our study, we investigate the effect of injury on the stellate neurons of the amygdala in a mouse model of mild bTBI using Golgi staining and dendritic analysis. This model recapitulates the injuries experienced by humans exposed to an explosive blast and we have shown previously (Rubovitch et al. 2011; Tweedie et al. 2013). With this model we found evidence of increased dendritic spine density and increased branching in the amygdalar neurons of TBI exposed mice, providing a possible explanation for the hyperactivity within this region seen in PTSD patients.

2. Materials and methods

2.1. Animal husbandry

Male ICR mice weighing 25–30 g were kept five per cage under a constant 12 h light/dark cycle at room temperature. Food and water were available ad libitum. For experimental group, at least 6 different mice were used. The ethics committee of the Sackler Faculty of Medicine approved the experimental protocol, in compliance with the guidelines for animal experimentation of the National Institutes of Health.

2.2. Blast trauma model

The blast-induced procedures took place in the experimental site of "Tamar Explosives" and of "Sadwin Consultancy" in central Israel (Rubovitch et al. 2011). Mice (both blast and sham) were anesthetized with an i.p. mixture of ketamine (100 mg/kg) and xylazine (10 mg/kg), a combination that induces deep anesthesia and still enables spontaneous respiration. Mice were held in a restricted plastic net in a holder clamped to the floor with screws, which fixed their position but did not protect them from the blast (Fig. 1A). Tied to each holder next to the mouse was a gauge, measuring blast levels (in PSI) and temperature. The explosion device was constructed as a cast of 500 g TNT. We used different distances between the explosive device and the animals in order to obtain different levels of blast intensity (Fig. 1B). The mice at a distance of 4 m were exposed to 5.5 psi peak over-pressure. The animals, pressure gauges and the explosive charges were elevated 1.0 m
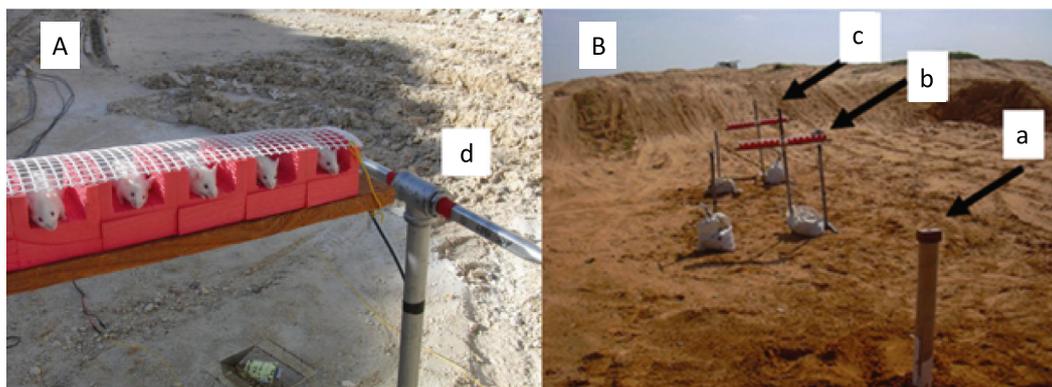

Fig. 1. Mouse model of mild blast TBI. (A) Anesthetized mice were held in a plastic net in a holder at a distance of 4 m from an explosive charge containing 500 g TNT. The explosion generates approximately 5.5 psi peak over-pressure at the 4 m distance. The measured peak over-pressure for this experiment was 37.9 kPa (5.4969 psi). The animals, pressure gauges and the explosive charges were elevated 1.0 m above ground level. (B) The rows are situated 4 (b) and 7 (c) meters from the TNT cast (a). Only the 4 m distance was used in this study. Each row had space for 12 mice and two pressure gauges were mounted at the ends of each platform (d). (Rubovitch et al. 2011).
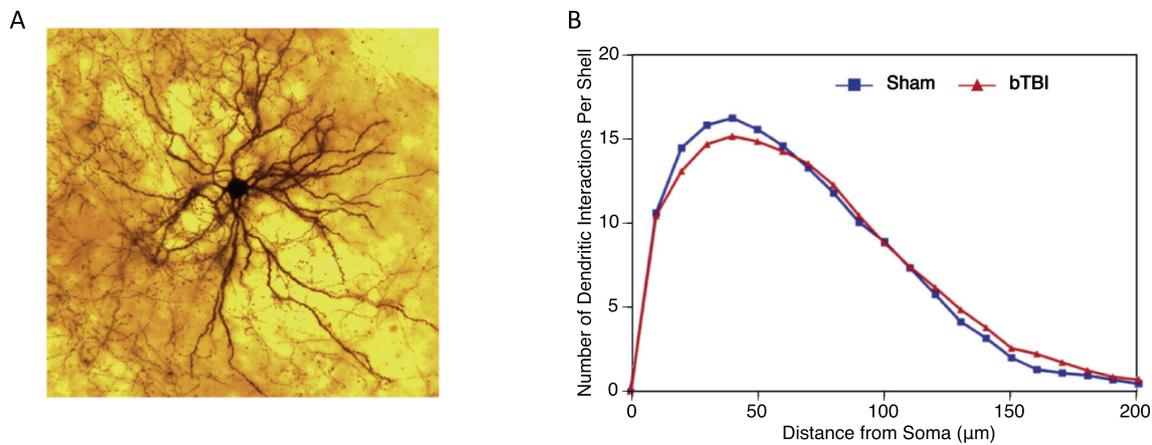
A

B

Fig. 2. Sholl analysis of amygdalar neurons. (A) A depiction of a typical amygdalar neuron's dendritic branching pattern is shown. (B) Sholl analysis is used to depict the distribution of the dendritic arbor at increasing distances from the soma. We found no significant differences in control (n = 6, 33 total neurons analyzed) and bTBI (n = 6, 36 total neurons analyzed) mice with regard to dendritic distribution (p = .514).

above ground level. All animals used in this experiment were exposed to a single explosion, on the same trial, such that all experimental parameters are equal. Each animal was anatomically positioned such that the angle and distance relative to the blast was identical. The pressures at both distances were measured 'side-on' with Free-Field ICP® Blast Pressure Sensor "pencil gauges" (PCB Piezoelectronics, Depew, NY, USA; Model 137). The recorded blast waves showed the "direct" shock wave and the reflected wave from the ground, as expected. There was also a reflected wave from the embankment surrounding the arena that was insignificant relative to the direct and ground reflected pressure waves. The sampling rate was 61.25 kHz or 16 microseconds between readings on all channels. The pressure-time curves were recorded for each experiment.

2.3. Dendritic analysis

Phosphate buffered saline followed by 4% neutral buffered formalin was used to perfuse mice 72 h days post injury. Brains were placed in 10% formalin overnight at 4 °C and then cryoprotected in 15% sucrose for 24 h. Formalin-fixed tissue blocks (2–3 mm thick in the coronal plane) incorporated the cortical samples and were stained using the Rapid Golgi method. Fixed tissue blocks were first placed in potassium dichromate and osmium tetroxide for approximately 6 days, then transferred to 0.75% silver nitrate for approximately 40 h. Blocks were dehydrated using increasing concentrations of alcohol solutions and ethyl ether, and were then infiltrated with increasing concentrations of nitrocellulose solutions (5%, 10%, 20%, 30%; 1–2 days each). Blocks were then placed in plastic molds and hardened with chloroform vapors. Tissue sections were cut to a thickness of 120 μm in the coronal plane using an AO sliding microtome, cleared in alpha-terpineol, rinsed with xylene, and mounted on slides using Permount. Neurons selected for dendritic analysis had to meet very strict criteria. Selected neurons must have been well impregnated; branches must be totally unobscured by other neurons, glia, blood vessels, or undefined precipitate (a staining by-product), and the soma must have been located within the middle third of the section. Approximately 6 neurons were selected and analyzed per animal. A single blinded observer was used for the entire experiment. A Zeiss brightfield microscope with long-working distance oil-immersion objective lessee and drawing tubes was used to prepare camera lucida drawings for analysis.

Dendritic arbors were analyzed using either of two methods: the Sholl Analysis, which defines the amount and distribution of the dendritic arbor, as well as an estimate of the total dendritic length, and the dendritic Branch Point Analysis (BPA) which characterized the complexity of the arbor based on the number of branch points and dendritic

bifurcations within the dendritic domain, as previously described (Diamond et al. 2006). Additionally, soma sizes were measured using a digitizing tablet linked to the drawing tube of the microscope. We also evaluated the presence of various dendritic spine types using this method.

2.4. Statistical analysis

GraphPad Prism software was used for statistical analysis. Mean values are depicted ± standard deviation and were compared using the two tailed t-test. For Golgi analyses, the values of individual neurons were averaged per brain and statistical analyses considered each biological sample (brain) per group. For Sholl and Branch Point Analyses, the Wilcoxon signed-rank test was used. In both tests $p < .05$ indicates significance.

3. Results

3.1. Sholl analysis

A visual example of the dendritic arbor of an amygdalar neuron is shown in Fig. 2A. The Sholl analysis depicts the distribution of the dendritic arbor at increasing distances from the soma. The profile of the neurons from the control brains is in blue, and the profile of the neurons from the bTBI brains is in red. There is no difference between the two profiles. Thus, the bTBI paradigm had no significant effect on the amount and distribution of the dendritic arbors (Fig. 2B).

3.2. Dendritic length

The data from the Sholl analysis were used to generate an approximation of the total dendritic length (in microns). In this context, the average dendritic length of the Stellate cells (per brain) were 2017 ± 121um for the control (n = 33) and 2019 ± 125 for the bTBI mice (n = 36) (Fig. 3). Each data point represents the average length of approximately 6 neurons from the amygdala of that brain. There are no significant differences between the two groups. This would further confirm the notion that the mild blast did not modify the amount and/or distribution of the dendritic arbors of amygdalar neurons from the basolateral nucleus of the mouse.

3.3. Branch point analysis

The branch point analysis compares the number of dendritic branch bifurcations at increasing branch orders from the soma. A comparison
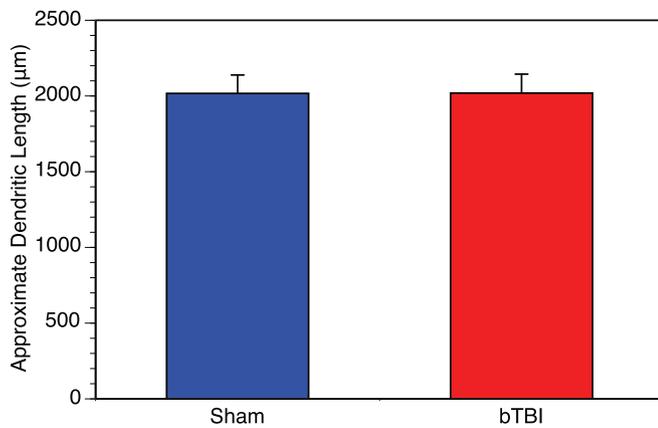
Fig. 3. Average dendritic length of amygdalar neurons. Dendritic length was measured and averaged for whole brain. We found no differences between the control (n = 6, 33 total neurons analyzed) and bTBI (n = 6, 36 total neurons analyzed) mice ($p = .992$). This indicates that blast does not appear to have an effect on dendritic length within the amygdala.
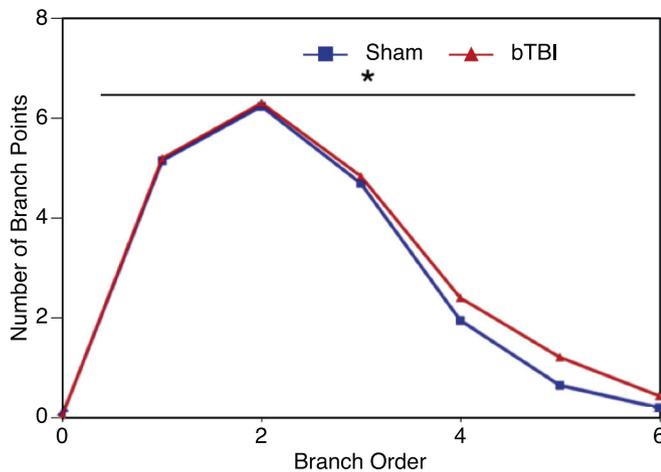

Fig. 4. Branch point analysis of amygdalar neurons. We utilized branch point analysis to evaluate the number of dendritic branch bifurcations at increasing orders from the soma. We showed that more distal portions (> 3 branch points) of the dendritic tree were significantly more complex in the bTBI (n = 6, 36 total neurons analyzed) mice compared to controls (n = 6, 33 total neurons analyzed) ($p = .031$).

of the profiles (Fig. 4) shows that there was significant difference ($p = .031$) between the two groups at the more distal portions (> 3 branch points) of the dendritic tree of the basolateral amygdalar neurons (e.g., the higher branch orders). There is more complexity of the dendritic tree of the bTBI neurons at these higher branch orders.

3.4. Soma size

The soma size of the entire basolateral amygdalar neurons was evaluated. Although, on a per brain level, the bTBI neurons had somas which were approximately 6% smaller than the controls, there was no significant difference between the two groups. The same results were seen per neuron as well (data not shown).

3.5. Total spine density

Dendritic spines were counted along three internal branch segments from each neuron. We quantified approximately 5 neurons per brain from each of the six brains in each group. When we evaluated spine density per neuron, the total spine density for the bTBI amygdalar
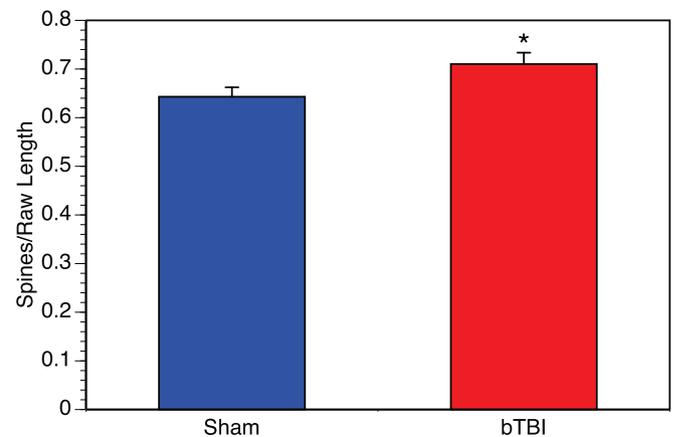

Fig. 5. Dendritic spine analysis of amygdalar neurons. To further evaluate morphological changes induced within the amygdala by blast TBI, we examined the density of dendritic spines on a per neuron basis. We saw significantly higher spine density among bTBI mice (n = 6, 31 total neurons analyzed) compared to controls (n = 6, 30 total neurons analyzed) ($p = .032$).

neurons were found to have significantly greater spine density, an approximately 10% increase (Fig. 5).

3.6. Spine configurations

In addition to the total dendritic spines, spine density was also evaluated in terms of specific spine configurations. Spines were characterized as either T-type (thin), M-type (mushroom), or S-type (stubby). Thin spines are characterized as having thin spine necks and a definitive spine head. They are often associated with learning phenomena and neuroplasticity. Mushroom spines – with a distinctive spine head and a thickened spine neck – have been more closely associated with memory functions. Finally, the small (S-type) spines – with no distinctive spine head or neck, and generally smaller than the T or M spines, has been associated with spine degeneration or dying-out.

3.6.1. T-type (thin) spines

No significant change was observed in the density of T-type spines in the basolateral amygdala on a per neuron (Fig. 6A) basis. Blast TBI did not appear to influence the T-type of dendritic spine within the basolateral amygdala.

3.6.2. M-type (mushroom) spines

M-type spines show a 27% increase in their spine density on a per neuron basis which was significant (Fig. 6B). This suggests that blast injury may be selectively increasing M-type spines.

3.6.3. S-type (stubby) spines

There was a small (+9%) increasing trend in stubby spines in the bTBI amygdalar neurons, per neuron (Fig. 6C), though this was not statistically significant. Although overall spine density did not change, this is suggestive of a possible increase in bTBI-related turnover of spines in the amygdala.

3.7. Result summary

While our mouse model of blast-related mild TBI did not induce significant changes in the amount and distribution of the dendritic arbor within the basolateral amygdala, we did see several interesting changes related to dendritic branching and spine density. We saw that, particularly at distal regions, there was more dendritic branching in the amygdala of bTBI exposed mice. We also saw increases in dendritic spine density with bTBI, with memory-related mushroom spines accounting for the majority of this increase. Overall, our model has
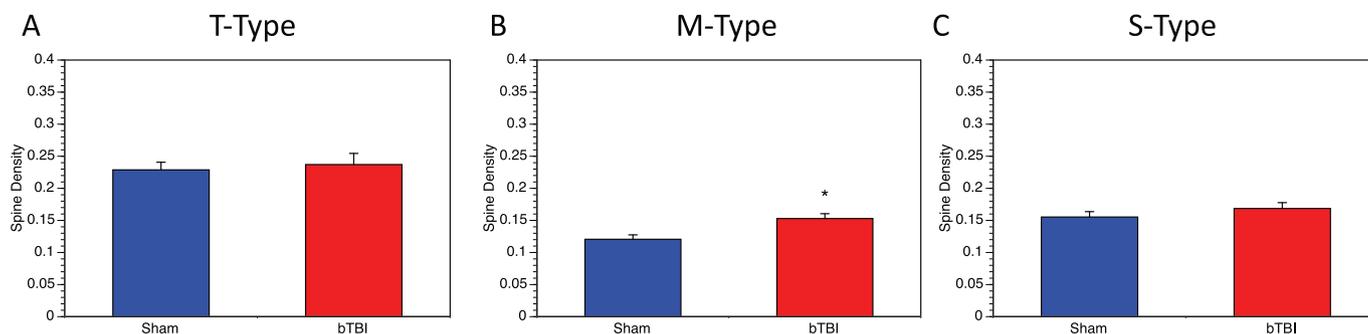
Fig. 6. Analysis of spine configurations. In addition to total spines, we also evaluated spine density based on three specific spine configurations on a per neuron basis in control (n = 6, 30 total neurons analyzed) and bTBI (n = 6, 31 total neurons analyzed) mice. (A) We examined T-type (thin) spines and saw no significant differences ($p = .695$). (B) M-type (mushroom) spines showed a significant increase in M-type spine density in bTBI mice ($p = .003$). (C) S-Type (stubby) spines showed small increases in density in bTBI, though this was not statistically significant ($p = .289$). A single control neuron outlier was removed from analysis of S-Type spines.

demonstrated increase connectivity within the amygdala as a result of exposure to mild blast trauma.

4. Discussion

Traumatic brain injury has become increasingly common, especially among combatants and civilians involved in recent conflicts. Among U.S. Forces, there have been approximately 384,000 brain injuries sustained since 2000 (Defense and Veterans Brain Injury Center 2018). Blast-related TBIs make up a significant portion of these injuries, especially within the context of training exercises and the increased use of IEDs (Hoge et al. 2008; Masel et al. 2012). TBI has also been linked as an important contributing factor to the development of PTSD (Hoge et al. 2008; Tanev et al. 2014). Previous experiments using our model of blast injury, at the same peak over-pressure, have yielded cognitive changes similar to that of both TBI and PTSD in humans, such as increased anxiety-like behaviors and deficits in spatial and recognition memory (Rachmany et al. 2017; Rubovitch et al. 2011). In this study, we have reproduced the effects of a blast TBI in a mouse model to better understand how mild bTBI may contribute to the development of PTSD through cellular changes within the amygdala.

Our model of blast TBI was mild, in that it did not produce significant changes in dendritic amount and distribution or soma size within the amygdala. We did, however, note changes in dendritic branching at more distal regions. Our branch point analysis showed significantly more branching distally in the bTBI exposed mice. This increased branching of stellate neurons may be indicative of increased communication within the amygdala. Similar increases in plasticity was observed in a recent model of fluid percussion injury in the rat (Hoffman et al. 2017), as well as in rodent models of stress alone (Lau et al. 2017; Vyas et al. 2002). This represents an important connection between the morphological changes associated with TBI and that of stress within the amygdala.

We also noted significant increases in dendritic spine density in the stellate neurons of the amygdala in mice exposed to bTBI. This increase in amygdalar dendritic spines has been observed previously in rodent models of chronic stress and depression (Mitra et al. 2005; Qiao et al. 2016; Qin et al. 2011) and that these increases in spine density correlate with deficits in fear extinction (Maroun et al. 2013). This suggests that the increase in dendritic spine density that we observed following bTBI may be representative of an amygdalar morphology similar to that which is observed following stress. Further, this morphological change may provide an explanation for the associated behavioral changes indicative of PTSD.

In order to better understand the specific morphological changes leading to this increase in dendritic complexity, we evaluated the distribution of dendritic spine types, including: T-type (thin), M-type

(mushroom), and S-Type (stubby). While we did not see significant changes in T and S-Type spines, we can attribute the increases in dendritic spine density in bTBI mice mainly to increases in M-type spines. This result is consistent with a rodent previous model of acute stress (Maroun et al. 2013), which showed its most pronounced spine increases in the M-type. These spines have been associated with more stable memory functions (Bourne and Harris 2007; Kasai et al. 2003) and have been suggested to contribute to increases in stress-induced basolateral amygdala hyperexcitability observed previously (Chauveau et al. 2012).

Using our mouse model of mild blast TBI, we have been able to identify several morphological changes within the stellate neurons of the basolateral amygdala which may provide an important connection between the physical trauma of TBI and the neurological symptoms of PTSD. It has been shown in previously that increased activity of the noradrenaline within the amygdala may contribute to the hyperarousal seen in PTSD (Ronzoni et al. 2016). The increased connectivity we have observed in our model may represent a means by which this noradrenaline signaling is enhanced. While previous studies have shown similar amygdalar changes in rodent models of chronic and acute stress and in a fluid percussion models, our study provides the first data on these changes in a rodent model of blast TBI. Overall, our model has shown that blast TBI induces changes that are suggestive of increased communication and memory functions within the amygdala, both of which could provide a foundation for PTSD-like behavioral changes. Further study of this model will help us better understand how changes within the amygdala following blast TBI can lead to or enhance comorbid PTSD and how we can identify treatments to prevent these changes from progressing.

Acknowledgements

Author disclosure

References

Admon, R., Lubin, G., Stern, O., Rosenberg, K., Sela, L., Ben-Ami, H., Hendler, T., 2009. Human vulnerability to stress depends on amygdala's predisposition and

hippocampal plasticity. Proc. Natl. Acad. Sci. U. S. A. 106, 14120–14125.

Admon, R., Leykin, D., Lubin, G., Engert, V., Andrews, J., Pruessner, J., Hendler, T., 2013. Stress-induced reduction in hippocampal volume and connectivity with the ventromedial prefrontal cortex are related to maladaptive responses to stressful military service. Hum. Brain Mapp. 34, 2808–2816.

Ahmed-Leitao, F., Spies, G., van den Heuvel, L., Seedat, S., 2016. Hippocampal and amygdala volumes in adults with posttraumatic stress disorder secondary to childhood abuse or maltreatment: a systematic review. Psychiatry Research. Neuroimaging 256, 33–43.

American Psychiatric Association, 2013. Diagnostic and Statistical Manual of Mental Disorders, 5th ed. (Washington, DC).

Andreasen, N.C., 2014. Acute and delayed posttraumatic stress disorders: a history and some issues. Am. J. Psychiatry 161, 1321–1323.

Bogdanova, Y., Verfaellie, M., 2012. Cognitive sequelae of blast-induced traumatic brain injury: recovery and rehabilitation. Neuropsychol. Rev. 22 (1), 4–20.

Bourne, J., Harris, K.M., 2007. Do thin spines learn to be mushroom spines that remember? Curr. Opin. Neurobiol. 17, 381–386.

Casella, E.M., Thomas, T.C., Vanino, D.L., Fellows-Mayle, W., Lifshitz, J., Card, J.P., Adelson, P.D., 2014. Traumatic brain injury alters long-term hippocampal neuron morphology in juvenile, but not immature, rats. Childs Nerv. Syst. 30, 1333–1342.

Chauveau, F., Lange, M.D., Jungling, K., Lesting, J., Seidenbecher, T., Pape, H.C., 2012. Prevention of stress-impaired fear extinction through neuropeptide s action in the lateral amygdala. Neuropsychopharmacology 37, 1588–1599.

Defense and Veterans Brain Injury Center, 2018. In: Defense, D.o (Ed.), DOD worldwide numbers for TBI, pp. 1–5 (Washington, DC).

Diamond, D.M., Campbell, A.M., Park, C.R., Woodson, J.C., Conrad, C.D., Bachstetter, A.D., Mervis, R.F., 2006. Influence of predator stress on the consolidation versus retrieval of long-term spatial memory and hippocampal spinogenesis. Hippocampus 16, 571–576.

Gao, X., Deng, P., Xu, Z.C., Chen, J., 2011. Moderate traumatic brain injury causes acute dendritic and synaptic degeneration in the hippocampal dentate gyrus. PLoS One 6, e24566.

Hoffman, A.N., Paode, P.R., May, H.G., Ortiz, J.B., Kemmou, S., Lifshitz, J., Conrad, C.D., Currier Thomas, T., 2017. Early and persistent dendritic hypertrophy in the basolateral amygdala following experimental diffuse traumatic brain injury. J. Neurotrauma 34, 213–219.

Hoge, C.W., McGurk, D., Thomas, J.L., Cox, A.L., Engel, C.C., Castro, C.A., 2008. Mild traumatic brain injury in U.S. soldiers returning from Iraq. N. Engl. J. Med. 358, 453–463.

Jackson, C.E., Green, J.D., Bovin, M.J., Vasterling, J.J., Holowka, D.W., Ranganathan, G., Rosen, R.C., Keane, T.M., Marx, B.P., 2016. Mild traumatic brain injury, PTSD, and psychosocial functioning among male and female U.S. OEF/OIF veterans. J. Trauma. Stress. 29, 309–316.

Kaplan, G.B., Leite-Morris, K.A., Wang, L., Rumbika, K.K., Heinrichs, S.C., Zeng, X., Wu, L., Arena, D.T., Teng, Y.D., 2018. Pathophysiological bases of comorbidity: traumatic brain injury and post-traumatic stress disorder. J. Neurotrauma 35, 210–225.

Kasai, H., Matsuzaki, M., Noguchi, J., Yasumatsu, N., Nakahara, H., 2003. Structure-stability-function relationships of dendritic spines. Trends Neurosci. 26, 360–368.

Koyama, Y., Nishida, T., Tohyama, M., 2013. Establishment of an optimised protocol for a Golgi-electron microscopy method based on a Golgi-Cox staining procedure with a commercial kit. J. Neurosci. Methods 218, 103–109.

Lau, T., Bigio, B., Zelli, D., McEwen, B.S., Nasca, C., 2017. Stress-induced structural plasticity of medial amygdala stellate neurons and rapid prevention by a candidate antidepressant. Mol. Psychiatry 22, 227–234.

Maroun, M., Ioannides, P.J., Bergman, K.L., Kavushansky, A., Holmes, A., Wellman, C.L., 2013. Fear extinction deficits following acute stress associate with increased spine density and dendritic retraction in basolateral amygdala neurons. Eur. J. Neurosci. 38, 2611–2620.

Masel, B.E., Bell, R.S., Brossart, S., Grill, R.J., Hayes, R.L., Levin, H.S., Rasband, M.N.,

Ritzel, D.V., Wade, C.E., DeWitt, D.S., 2012. Galveston Brain Injury Conference 2010: clinical and experimental aspects of blast injury. J. Neurotrauma 29, 2143–2171.

Mitra, R., Jadhav, S., McEwen, B.S., Vyas, A., Chattarji, S., 2005. Stress duration modulates the spatiotemporal patterns of spine formation in the basolateral amygdala. Proc. Natl. Acad. Sci. U. S. A. 102, 9371–9376.

Pitman, R.K., Shin, L.M., Rauch, S.L., 2001. Investigating the pathogenesis of posttraumatic stress disorder with neuroimaging. J. Clin. Psychiatry 62 (Suppl. 17), 47–54.

Qiao, H., Li, M.X., Xu, C., Chen, H.B., An, S.C., Ma, X.M., 2016. Dendritic spines in depression: what we learned from animal models. Neural Plast. 2016, 8056370.

Qin, M., Xia, Z., Huang, T., Smith, C.B., 2011. Effects of chronic immobilization stress on anxiety-like behavior and basolateral amygdala morphology in Fmr1 knockout mice. Neuroscience 194, 282–290.

Rachmany, L., Tweedie, D., Rubovitch, V., Li, Y., Holloway, H.W., Kim, D.S., Ratliff, W.A., Saykally, J.N., Citron, B.A., Hoffer, B.J., Greig, N.H., Pick, C.G., 2017. Exendin-4 attenuates blast traumatic brain injury induced cognitive impairments, losses of synaptophysin and in vitro TBI-induced hippocampal cellular degeneration. Sci. Rep. 7, 3735.

Rauch, S.L., Shin, L.M., Phelps, E.A., 2006. Neurocircuitry models of posttraumatic stress disorder and extinction: human neuroimaging research–past, present, and future. Biol. Psychiatry 60, 376–382.

Ronzoni, G., Del Arco, A., Mora, F., Segovia, G., 2016. Enhanced noradrenergic activity in the amygdala contributes to hyperarousal in an animal model of PTSD. Psychoneuroendocrinology 70, 1–9.

Rubovitch, V., Ten-Bosch, M., Zohar, O., Harrison, C.R., Tempel-Brami, C., Stein, E., Hoffer, B.J., Balaban, C.D., Schreiber, S., Chiu, W.T., Pick, C.G., 2011. A mouse model of blast-induced mild traumatic brain injury. Exp. Neurol. 232, 280–289.

Sajja, V.S., Hubbard, W.B., VandeVord, P.J., 2015. Subacute oxidative stress and glial reactivity in the amygdala are associated with increased anxiety following blast neurotrauma. Shock 1, 71–78.

Sartory, G., Cwik, J., Knuppertz, H., Schurholt, B., Lebens, M., Seitz, R.J., Schulze, R., 2013. In search of the trauma memory: a meta-analysis of functional neuroimaging studies of symptom provocation in posttraumatic stress disorder (PTSD). PLoS One 8, e58150.

Saykally, J.N., Ratliff, W.A., Keeley, K., Pick, C.G., Mervis, R.F., Citron, B.A., 2017. Repetitive mild closed head injury alters protein expression and dendritic complexity in a mouse model. J. Neurotrauma 35, 139–148.

Seedat, S., Warwick, J., van Heerden, B., Hugo, C., Zungu-Dirwayi, N., Van Kradenburg, J., Stein, D.J., 2004. Single photon emission computed tomography in posttraumatic stress disorder before and after treatment with a selective serotonin reuptake inhibitor. J. Affect. Disord. 80, 45–53.

Shin, L.M., Liberzon, I., 2010. The neurocircuitry of fear, stress, and anxiety disorders. Neuropsychopharmacology 35, 169–191.

Tanev, K.S., Pentel Kz Fau - Kredlow, M.A., Kredlow, Ma, Fau - Charney, M.E., Charney, M.E., 2014. PTSD and TBI co-morbidity: scope, clinical presentation and treatment options. Brain Inj. 261–270.

Tweedie, D., Rachmany, L., Rubovitch, V., Zhang, Y., Becker, K.G., Perez, E., Hoffer, B.J., Pick, C.G., Greig, N.H., 2013. Changes in mouse cognition and hippocampal gene expression observed in a mild physical- and blast-traumatic brain injury. Neurobiol. Dis. 54, 1–11.

VanElzakker, M.B., Dahlgren, M.K., Davis, F.C., Dubois, S., Shin, L.M., 2014. From Pavlov to PTSD: the extinction of conditioned fear in rodents, humans, and anxiety disorders. Neurobiol. Learn. Mem. 113, 3–18.

Vyas, A., Mitra, R., Shankaranarayana Rao, B.S., Chattarji, S., 2002. Chronic stress induces contrasting patterns of dendritic remodeling in hippocampal and amygdaloid neurons. J. Neurosci. 22, 6810–6818.

Winston, C.N., Chellappa, D., Wilkins, T., Barton, D.J., Washington, P.M., Loane, D.J., Zapple, D.N., Burns, M.P., 2013. Controlled cortical impact results in an extensive loss of dendritic spines that is not mediated by injury-induced amyloid-beta accumulation. J. Neurotrauma 30, 1966–1972.